Electronic Supplementary Information

Luminescence Detection of CH_2Cl_2 via Varying Cu···Cu Interaction in a Flexible Porous Coordination Polymer

Wei-Jie Zhang#,[a] Wan-Tao Chen#,[a] Chen-Hui Li,[a] Wen-Zhu Sun,[a] Jia-Wen Ye*,[a] Ling Chen*,[a] Hai-Ping Wang*,[a] Xiao-Ming Chen.[b]

[a]School of Biotechnology and Health Sciences, Wuyi University, Jiangmen, Guangdong 529000, PR China.

[b]MOE Key Laboratory of Bioinorganic and Synthetic Chemistry, School of Chemistry, Sun Yat-Sen University, Guangzhou 510275, PR China.

#These authors contributed equally.

EXPERIMENTAL DETAILS

General Methods

DFT calculations. The binding energy was calculated by Dmol3 module of Materials Studio 8.0 software package. The Perdew-Burke-Ernzerhof (PBE) generalized gradient approximation (GGA) exchange–correlation functional with the double numeric plus (DNP) polarization basis set was utilized.[1] The effective core potentials were used. Grimme semiempirical methods to describe the long-range van der Waals interactions. The DFT-D are employed to the dispersion correction.[2] The convergence tolerance was as follows: 10^{-5} Ha (Energy), 0.002 Ha/Å (Max. force) and 0.005 Å (Max. displacement). The binding energy (ΔE) was computed by the following equation: $\Delta E = E$ (**CP**, without guest) + E (guest) – E (**CP**, with guest). The calculation results are shown in Table S2.
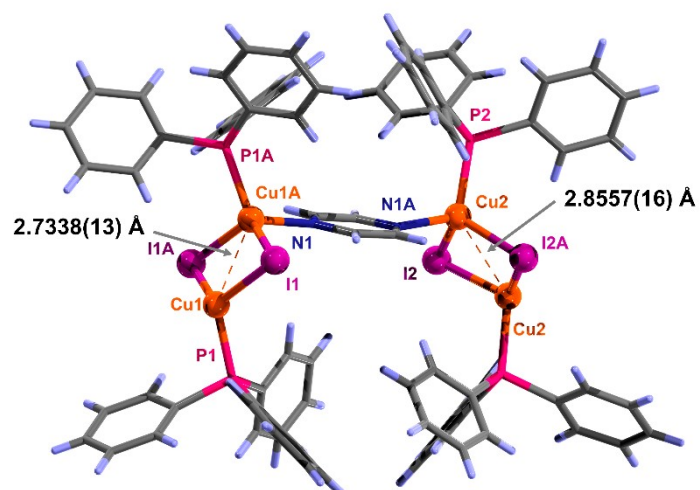
Fig. S1. The Cu···Cu distances in **CIPP** at room temperature. Color code: Cu, orange; I, purple; N, indigo; P, pink; C, gray; H, light purple.
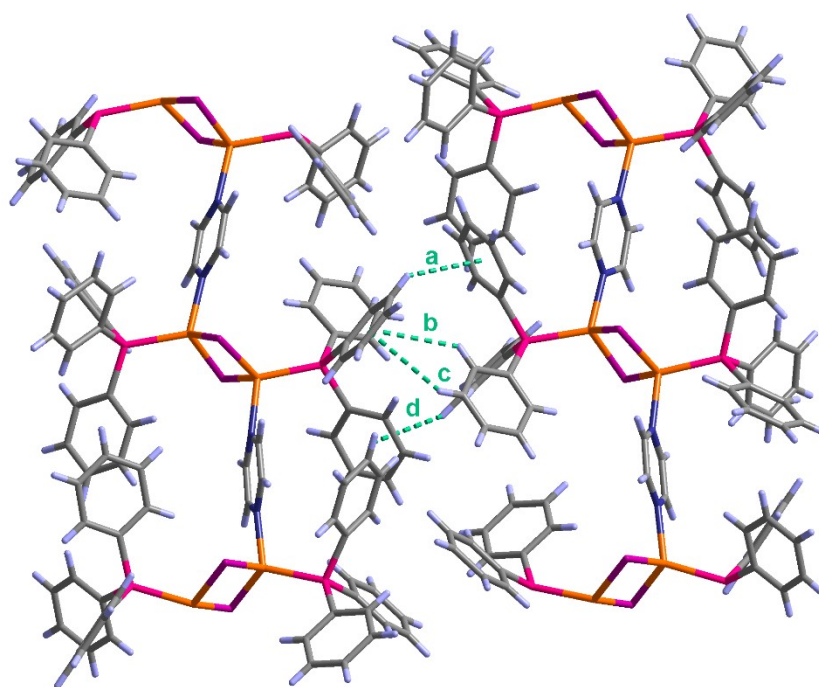

Fig. S2. The 1D chains in **CIPP** that are stacked by C–H···π interactions. Color codes: Cu, orange; I, purple; N, indigo; P, pink; C, gray; H, light purple. Green dotted line, C–H···π. a, 3.04 Å; b, 3.31 Å; c, 3.50 Å; d, 3.45 Å.
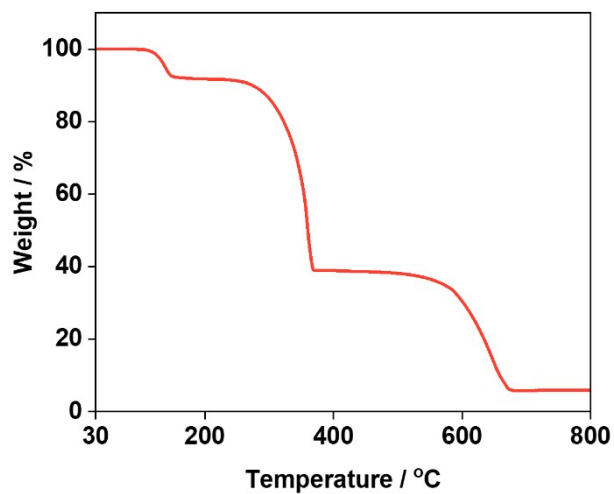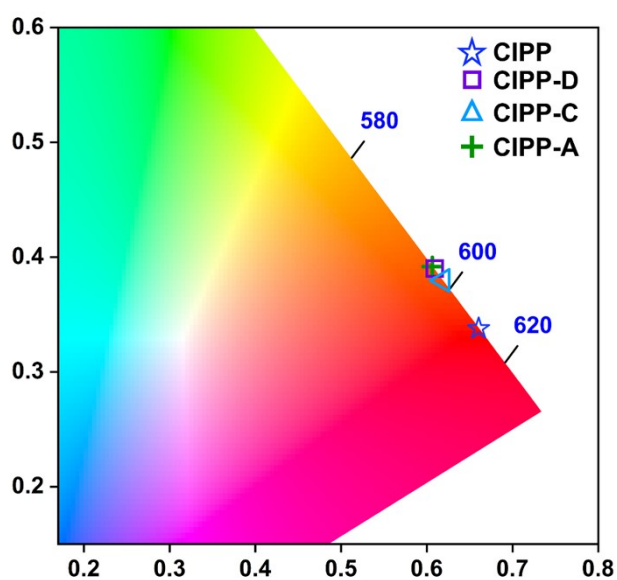
Fig. S3. The TG curve of **CIPP**.

Fig. S4. CIE coordinates of **CIPP**, **CIPP-D**, **CIPP-C** and **CIPP-A**, respectively.
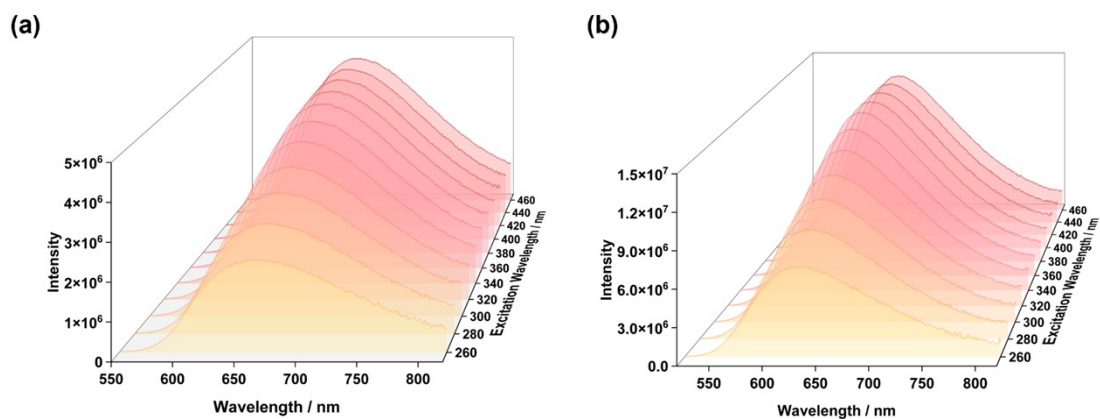

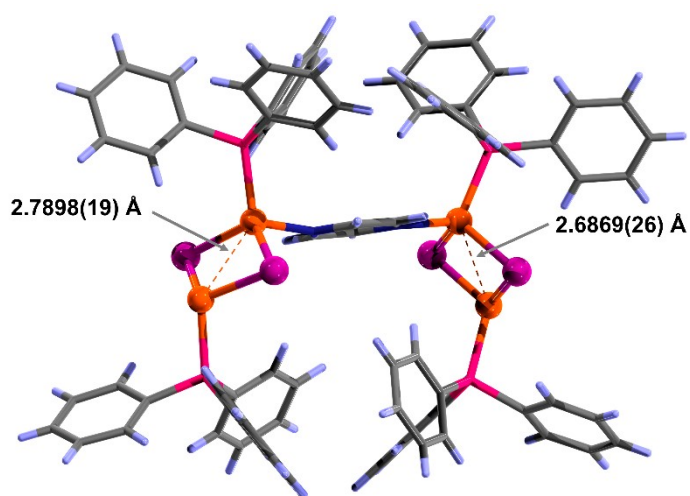**Fig. S5.** The excitation-emission maps of (a) **CIPP** and (b) **CIPP-D**.

Fig. S6. The Cu···Cu distances in **CIPP** at 150 K. Color codes: Cu, orange; I, purple; N, indigo; P, pink; C, gray; H, light purple.
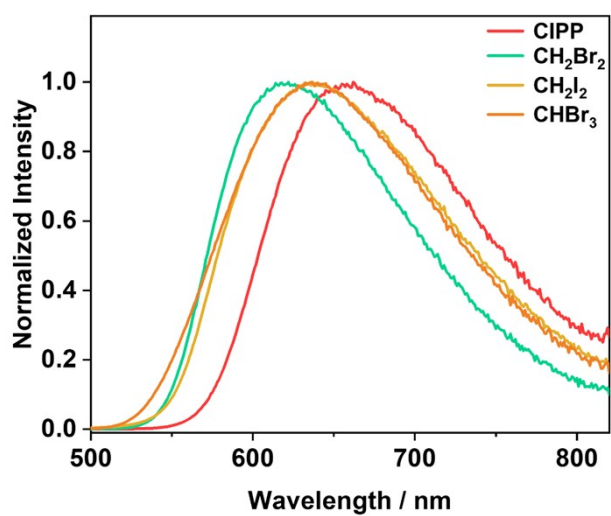

Fig. S7. The emission spectra of **CIPP** after exposure in different halohydrocarbon vapor, excited at 365 nm. The λ_{em} locates at 622, 638 and 640 nm after exposure in CH_2Br_2, CH_2I_2, $CHBr_3$, respectively.
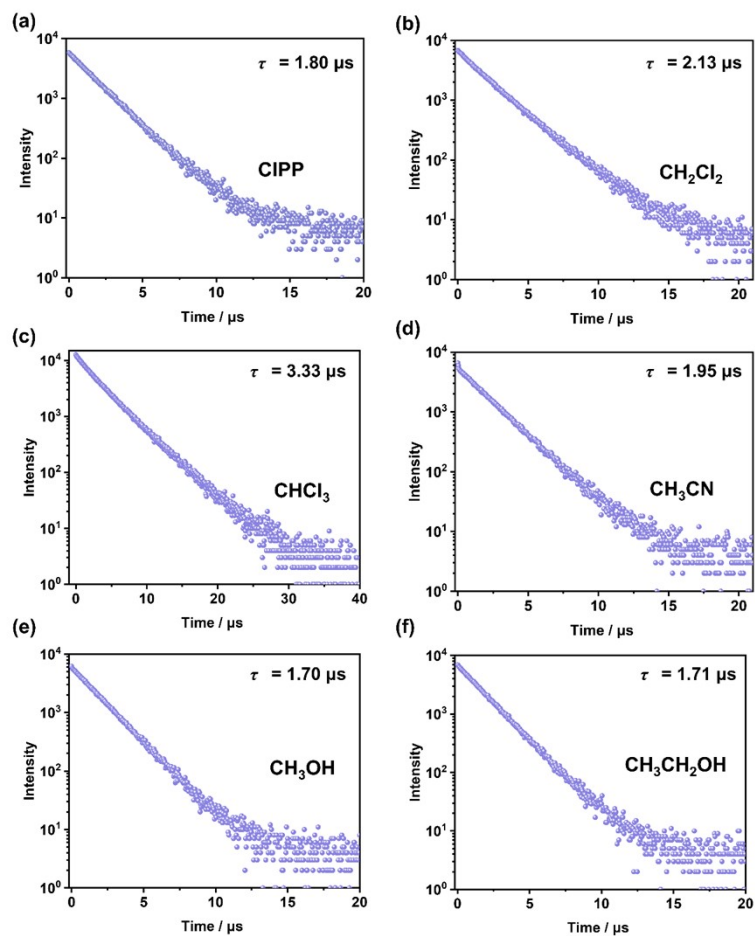
Fig. S8. The decay curves of **CIPP** before and after exposure in different vapors, excited by 375-nm VPL and detected at λ_{em}.
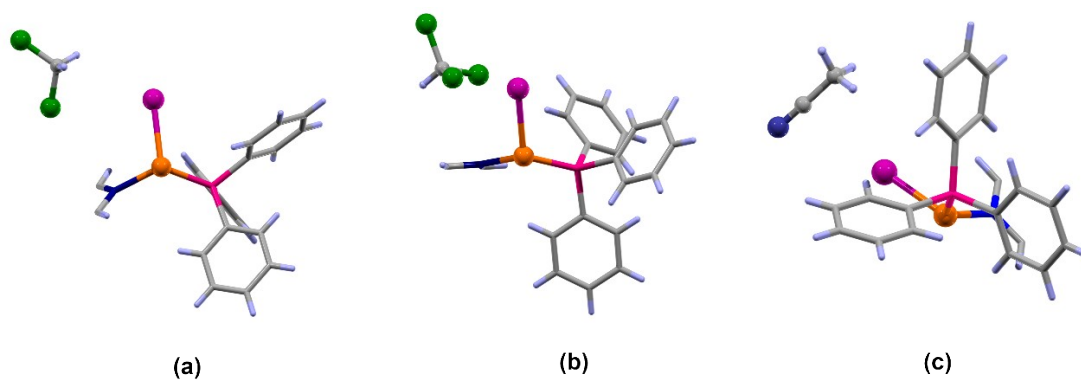

(a)   (b)   (c)

Fig. S9. The asymmetric units of (a) **CIPP-D**, (b) **CIPP-C** and (c) **CIPP-A**, respectively. Color codes: Cu, orange; I, purple; Cl, green; N, indigo; P, pink; C, gray; H, light purple.
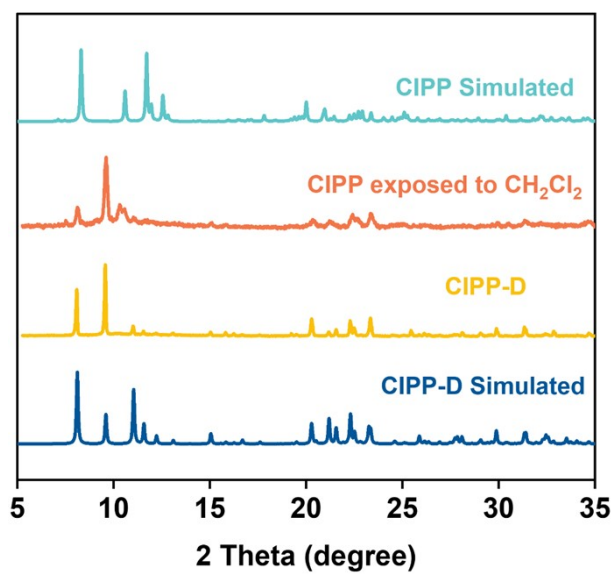
Fig. S10. PXRD patterns of the as-synthesized **CIPP-D** and **CIPP** was exposed in saturated CH_2Cl_2 vapor for 3 hours, respectively.
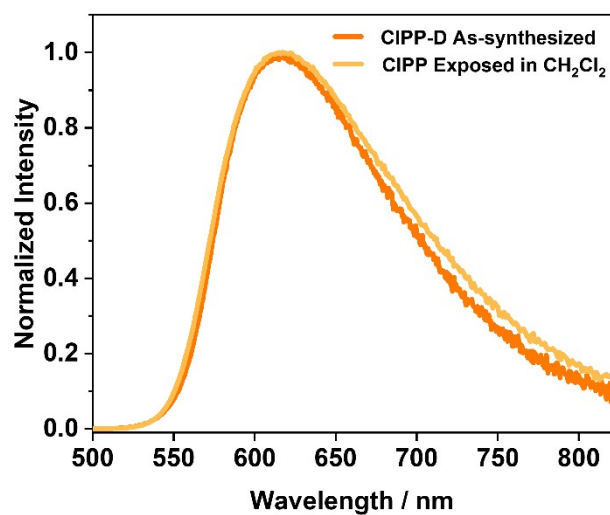

Fig. S11. Emission spectra of the as-synthesized **CIPP-D** and **CIPP** powder after exposure in CH_2Cl_2 vapor, excited at 365 nm.
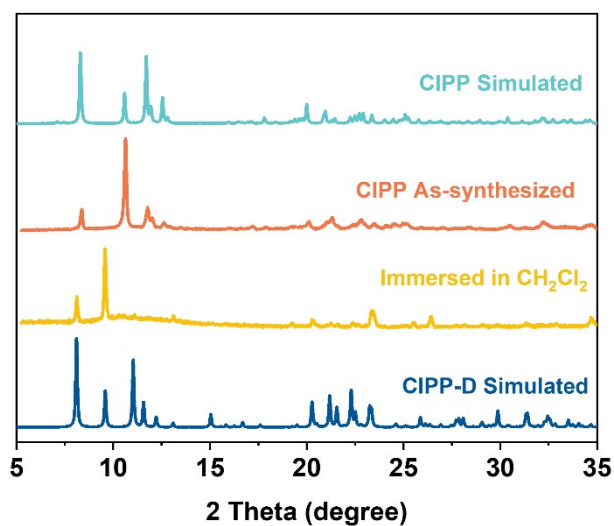
Fig. S12. PXRD patterns of **CIPP** before and after immersing in CH_2Cl_2 solvent.

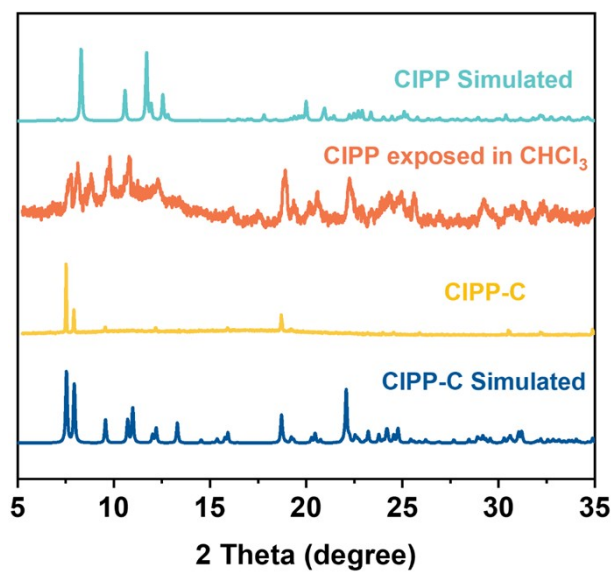**Fig. S13.** PXRD patterns of **CIPP** before and after exposure in $CHCl_3$ saturated vapor for 3 h.
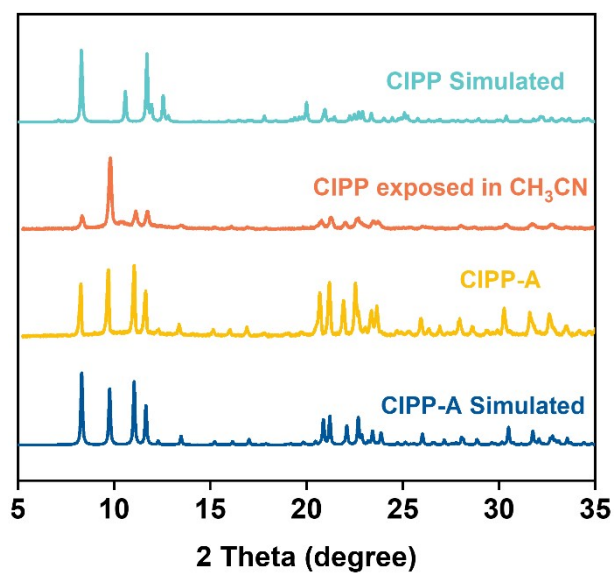
Fig. S14. PXRD patterns of the as-synthesized **CIPP-A** and **CIPP** after exposure in saturated CH_3CN vapor for 3 hours, respectively.
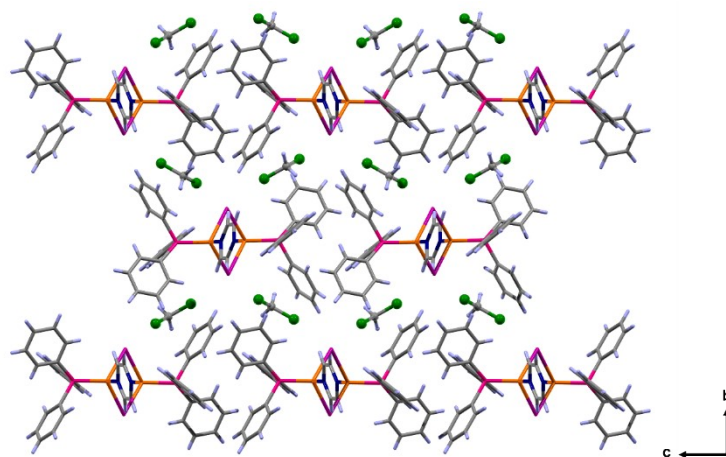
Fig. S15. The stacking mode of chains in **CIPP-D** along the *a*-axis. Color codes: Cu, orange; I, purple; Cl, green; N, indigo; P, pink; C, gray; H, light purple.

Fig. S16. The chain stacking by C–H···π interaction between triphenylphosphine ligands in **CIPP-D**. a, 3.21 Å; b, 3.20 Å; c, 3.38 Å; d, 3.49 Å; e, 3.20 Å; f, 3.21 Å.

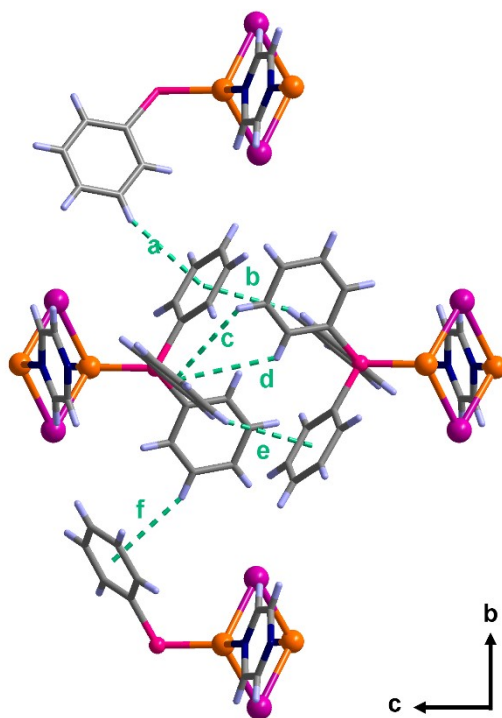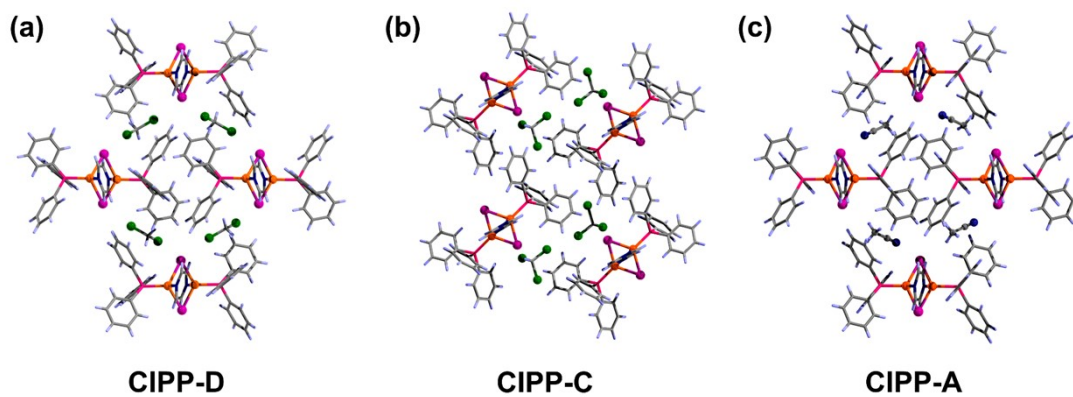**Fig.S17.** The guests that located in the cavities of (a) **CIPP-D**, (b) **CIPP-C**, and (c) **CIPP-A**, respectively. Color codes: Cu, orange; I, purple; Cl, green; N, indigo; P, pink; C, gray; H, light purple.
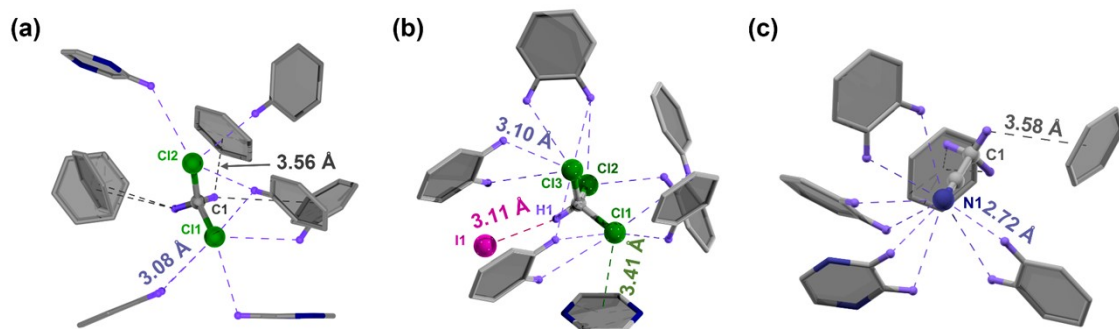
Fig. S18. Intramolecular interactions between guest molecules with the frameworks of (a) **CIPP-D**, (b) **CIPP-C** and (c) **CIPP-A**, respectively. The corresponding distances of interactions are shown in Table S3. Purple dotted line, Cl/N···H; green dotted line, Cl···π; grey dotted line, C–H···π; pink dotted line, I···H.
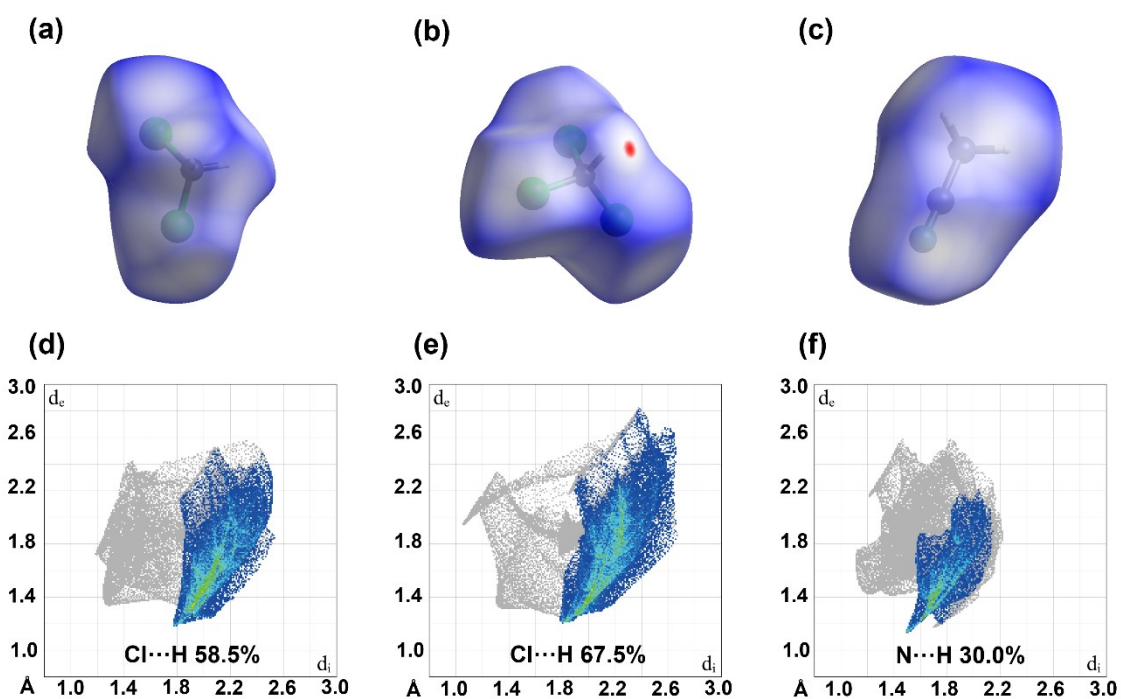
Fig. S19. Hirshfeld surfaces of (a) CH_2Cl_2 in **CIPP-D**, (b) $CHCl_3$ in **CIPP-C**, (c) CH_3CN in **CIPP-A**. The 2D fingerprint plots of Hirshfeld surfaces for (d) CH_2Cl_2, (e) $CHCl_3$ and (f) CH_3CN.
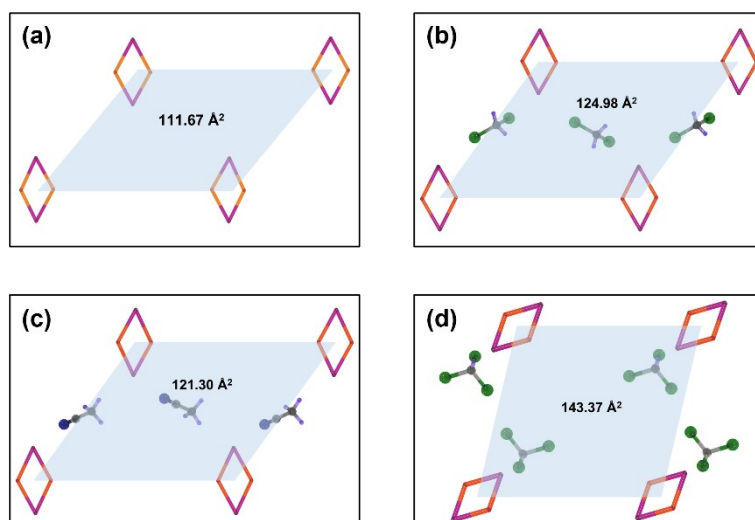
Fig. S20. The occupied areas of adjacent chains in (a) **CIPP**, (b) **CIPP-D**, (c) **CIPP-A**, (d) **CIPP-C**, respectively.
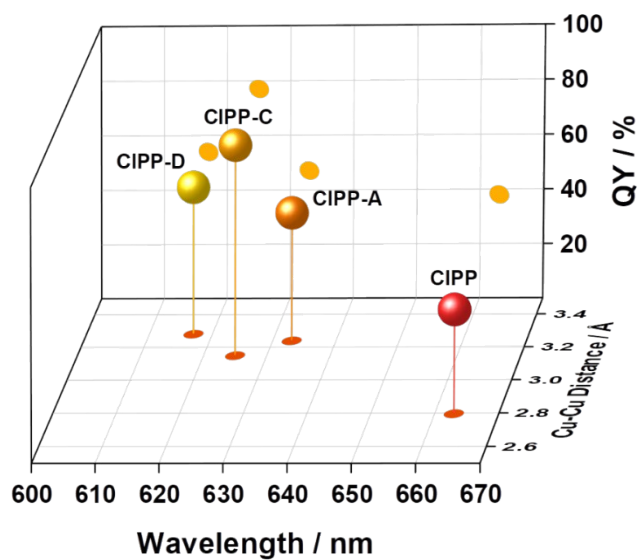
Fig. S21. Emission wavelengths, Cu···Cu distances and PLQYs of **CIPP**, **CIPP-D**, **CIPP-C** and **CIPP-A**, respectively.
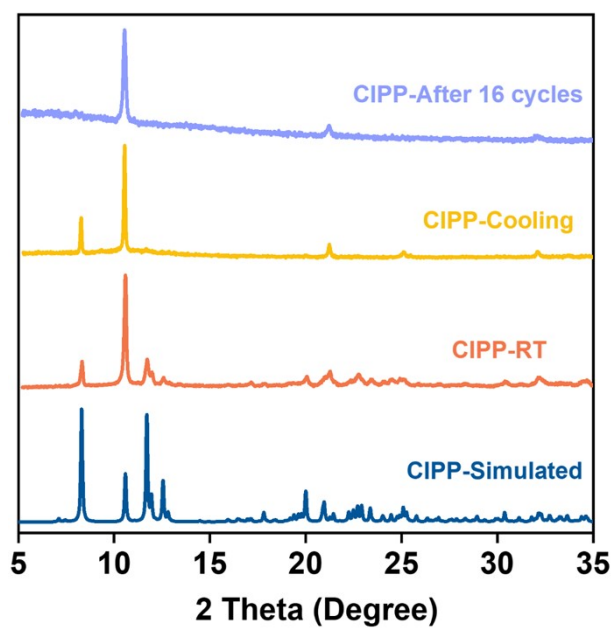
Fig. S22. PXRD patterns of the as-synthesized **CIPP** at room temperature (RT), **CIPP** that was heated at 318 K and then cooled to the room temperature, and after 16 heating/cooling cycles, respectively.
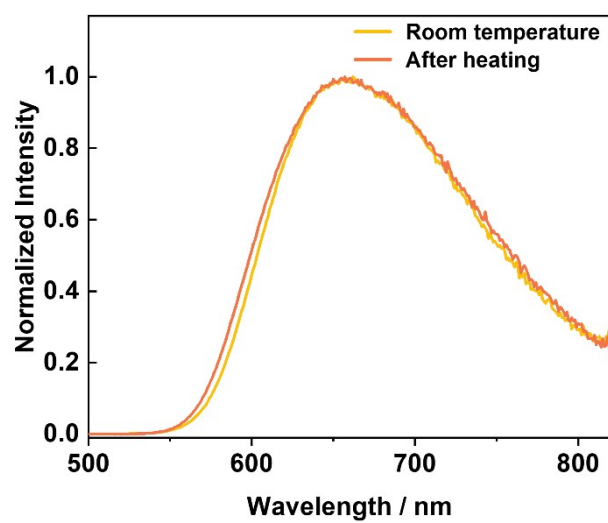
Fig. S23. Emission spectra of the as-synthesized **CIPP** and **CIPP** that was heated at 318 K and then cooled to the room temperature, respectively, excited at 365 nm.
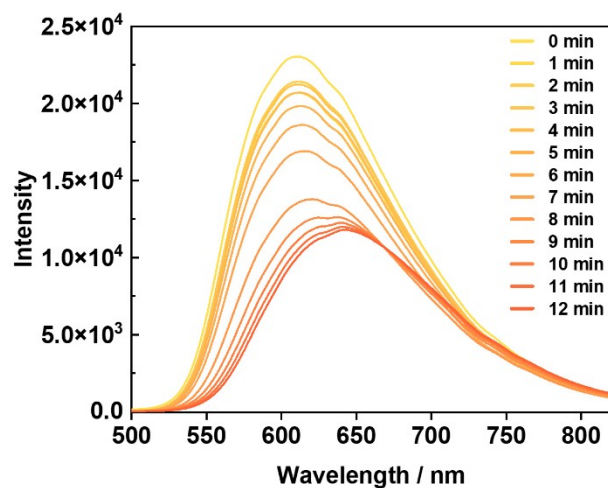
Fig. S24. Time-dependent emission spectra of spontaneous desorption of **CIPP-D** measured with a CCD detector, excited at 365 nm.
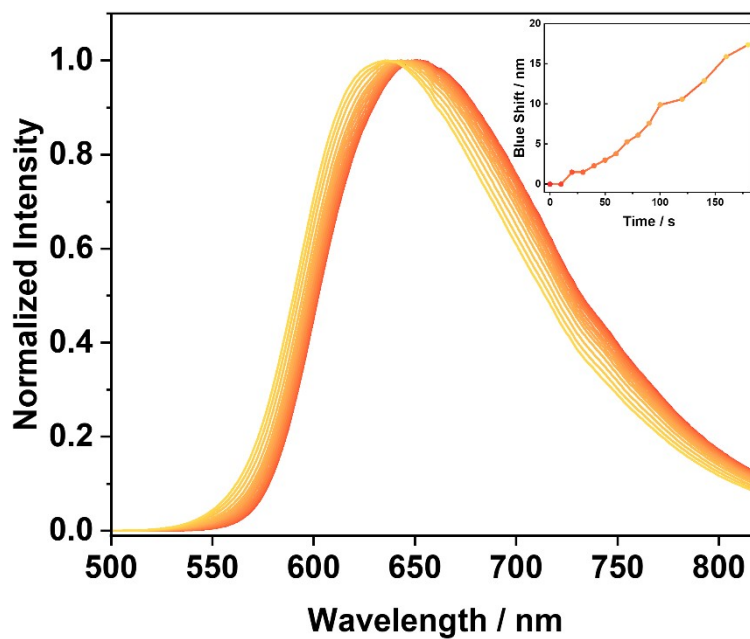
Fig. S25. Time-dependent emission spectra of **CIPP** in $CHCl_3$ saturated vapor, measured with a CCD detector, excited at 365 nm. Insert: Time-dependent blue shift of λ_{em}.

Fig. S26. Time-dependent emission spectra of **CIPP** in CH_3CN saturated vapor, measured with a CCD detector, excited at 365 nm. Insert: Time-dependent blue shift of λ_{em}.

Table S1. Crystallographic data and structure refinement parameters.

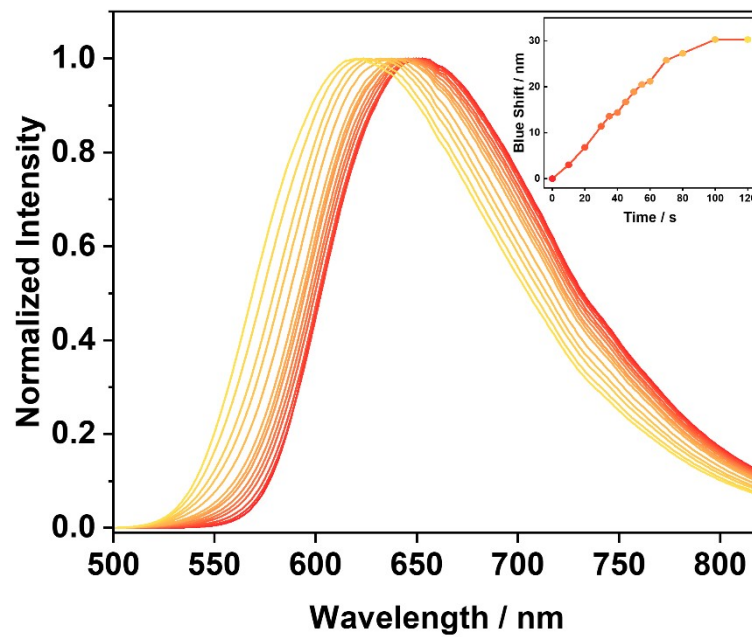| Compounds	CIPP	CIPP-150K	CIPP-D	CIPP-C	CIPP-A
Formula	$C_{60}H_{51}Cu_3I_3N_3P_3$	$C_{60}H_{51}Cu_3I_3N_3P_3$	$C_{21}H_{19}Cl_2CuINP$	$C_{21}H_{18}Cl_3CuINP$	$C_{22}H_{20}CuIN_2P$
Formula weight	1478.27	1478.27	577.68	612.12	533.81
T (K)	299.0(6)	150.00(10)	299.01(19)	298.83(10)	149.99(10)
Crystal system	Monoclinic	Monoclinic	Monoclinic	Triclinic	Monoclinic
Space group	$C2/c$	$I2/a$	$P2_1/n$	$P\text{-}1$	$P2_1/n$
a (Å)	29.6215(17)	28.0131(14)	8.9147(2)	8.82120(10)	8.9442(3)
b (Å)	16.6994(4)	16.5872(6)	18.4311(4)	12.1444(2)	18.0966(5)
c (Å)	28.2794(18)	27.2755(13)	13.5398(4)	12.2371(2)	13.1452(4)
α (°)	90	90	90	74.734(2)	90
β (°)	123.011(8)	115.762(6)	93.423(2)	69.225(2)	93.281(3)
γ (°)	90	90	90	83.1210(10)	90
V (Å^3)	11730.5(14)	11414.1(10)	2220.72(10)	1181.95(4)	2124.19(11)
Z	8	8	4	2	4
R_{int}	0.0528	0.0456	0.0457	0.0389	0.0538
[a]R_1 [$I \geq 2\sigma(I)$]	0.0492	0.0634	0.0385	0.0312	0.0370
[b]wR_2	0.1534	0.1954	0.1009	0.0840	0.0943
GOF	1.052	1.136	1.048	1.074	0.998

[a]$R_1 = \Sigma||F_o| - |F_c||/\Sigma|F_o|$.

[b]$wR_2 = [\Sigma w(F_o^2 - F_c^2)^2/\Sigma w(F_o^2)^2]^{1/2}$

Table S2. The binding energy of host-guest interaction.

E (**CIPP-D**) / kJ mol^{-1}	E (**CIPP-D** – CH_2Cl_2) / kJ mol^{-1}	E (CH_2Cl_2) / kJ mol^{-1}	ΔE / kJ mol^{-1}
−5992987.04	−3531718.70	−2461183.30	85.04

E (**CIPP-C**) / kJ mol^{-1}	E (**CIPP-C** – $CHCl_3$) / kJ mol^{-1}	E ($CHCl_3$) / kJ mol^{-1}	ΔE / kJ mol^{-1}
−7171664.96	−3531706.26	−3639862.70	96.00

E (**CIPP-A**) / kJ mol^{-1}	E (**CIPP-A** – CH_3CN) / kJ mol^{-1}	E (CH_3CN) / kJ mol^{-1}	ΔE / kJ mol^{-1}
−3872084.45	−3531725.88	−340272.90	85.67

Table S3. The host-guest interaction distances.

Compounds	Cl/N···H	C–H···π	Cl···π	I···H
CIPP-D	**Cl1···H / Å**			
	3.077			
	3.153			
	3.238	3.563		
	3.257	3.982	-	-
	3.334	4.121		
	Cl2···H / Å	4.172		
	3.315			
	3.333			
	3.354			
CIPP-C	**Cl1···H / Å**			
	3.408			
	3.464			
	3.495			
	Cl2···H / Å			
	3.307			
	3.151	-	3.414	3.108
	Cl3···H / Å			
	3.094			
	3.124			
	3.283			
	3.287			
	3.536			
CIPP-A	**N1···H / Å**			
	2.725			
	2.935	3.585		
	3.025	3.569	-	-
	3.041	3.755		
	3.062			
	3.068			
	3.377			

References

1 J. P. Perdew, K. Burke and M. Ernzerhof, Generalized Gradient Approximation Made Simple. *Phys. Rev. Lett.,* 1996, **77**, 3865-3868.

2 S. Grimme, Semiempirical GGA-type density functional constructed with a long-range dispersion correction, *J. Comput. Chem*., 2006, **27**, 1787-1799.